Journal of Engineering Mathematics **30:** 355–363, 1996.

Applications of conformal mapping to diverging open channel flows

SANJIV K. SINHA and A. JACOB ODGAARD
Department of Civil and Environmental Engineering and Iowa Institute of Hydraulic Research, The University of Iowa, Iowa City, IA 52242, U.S.A.

Received 29 March 1994; accepted in revised form 1 May 1995

Key words: Conformal mapping, diversion flows, Schwarz-Christoffel transformation, complex-physical transformation, hodograph plane, free streamline

Abstract. A conformal mapping technique is used for predicting the width of the separation zone at a diverging open channel flow. The Schwarz-Christoffel transformation is used to transform the physical boundaries of the flow into a complex plane and the flow field is solved using modified boundary conditions utilizing a complex velocity potential in the resulting hodograph plane. The final solution gives the width of the separation zone in nondimensionalized form and provides an inviscid solution for comparative study.

1. Introduction

Conformal mapping can be used for solving steady, two-dimensional potential flows with a free surface in which the flow is bounded partly by rigid walls and partly by free streamlines and gravity effects are negligible. Examples are flow of columns of liquids of finite lateral dimensions surrounded by gas ('unsubmerged' jets) and flow around bodies moving along the surface of a body of liquid otherwise at rest under gravity. The broad features of such flows can be discerned by momentum integral methods. However, the unknown shape of the free streamline makes obtaining an exact mathematical solution very difficult. If the boundaries of the flow field consist of piece-wise straight segments, the polygonal physical boundary can be mapped onto a complex plane. The solution then can be obtained by determining parametric relationships between the flow region in a hodograph plane and the transformed physical plane [1 (pp. 376–596), 2]. This technique has been applied previously to studies of jet efflux and deflection [3 (pp. 161–191)], transition flows [4], flow past a solid obstruction [5 (pp. 95–142)], and converging open channel flows [6] among others.

This paper presents the first such application to diverging open channel flows. Such flows occur both naturally as well as man-made. Because of irregular boundaries, naturally occurring diversion flows (e.g. alluvial river networks) often will have to be solved by using numerical modeling [7, 8]. However, man-made diversion flows usually contain piece-wise straight boundaries allowing for the application of conformal mapping techniques. A typical example of man-made diversion flow is flow into a water intake situated on the bank of the river. In this case, the flow diverges into two branches, one in the direction of the main channel and the other at an angle, α, to the main channel (Fig. 1). Another example is the storm sewer with diverging channel junctions. Steady, homogeneous, incompressible viscous flow past such junctions is typified by the presence of free streamlines of unknown shape along which the pressure can be taken to be constant.

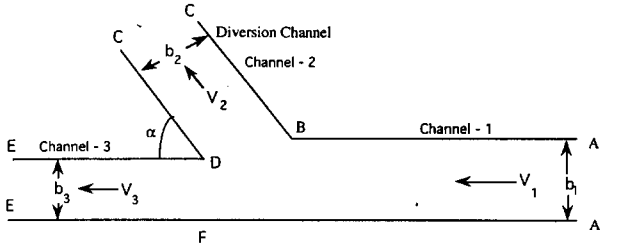

Fig. 1. Physical boundaries of channel junction (Z-plane).

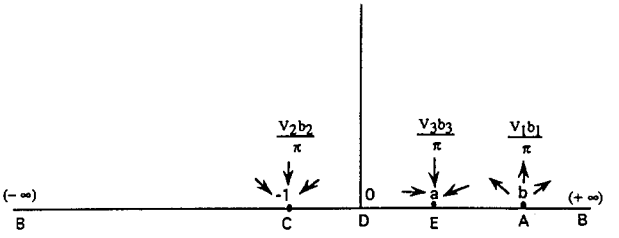

Fig. 2. Transformation layout for locating stagnation point (ξ-Plane).

The angle of diversion, α, is kept general. For the sake of simplicity, all the boundaries are assumed to be straight. The analysis is done in two steps. Step one involves transforming the physical plane into a complex plane using a Schwarz-Christoffel transformation. Next, the velocity field is transformed into the hodograph plane and the resulting equations are solved. Since this is a two-dimensional potential flow analysis, it is inherent in the analysis that the flow is irrotational and inviscid. While this is a major assumption, considering the fact that the flow at diversions is highly three dimensional with the secondary currents playing an important part in the generation of the structure and dimensions of the free streamline, the analysis is nonetheless useful as it gives the approximate lateral dimensions of the free streamlines and allows comparison with experimental data.

2. Analysis

The analysis parallels that of Ref. [6]. Initially, the position of the stagnation point in the flow is located, assuming that there is no free streamline. A free streamline will be incorporated later. The location of the stagnation point must be determined as per Ref. [6], so that the flow domain can be solved separately, depending on the location of the stagnation point. Hence, the cases considered are as follows:

2.1. Determination of the Stagnation Point

The actual flow plane, Z (Fig. 1), is transformed into a complex plane, ξ (Fig. 2), using the Schwarz-Christoffel transformation. Thereby, the flow field is divided into a polygon and the final transformation is done, using the limiting boundary conditions. The transformation required to map the flow domain on the upper side of the real axis is

$$\frac{dZ}{d\xi} = \frac{K\xi^{\alpha/\pi}}{(\xi - a)(\xi - b)(\xi + 1)} \tag{1}$$

where a and b are distances of points on real axis of ξ plane and K is a complex constant. Equation (1) can be simplified to

$$\frac{dZ}{d\xi} = K\xi^{(\alpha-\pi)/\pi} \times \left[\frac{a}{(1+a)(b-a)(a-\xi)} - \frac{1}{(1+a)(1+b)(\xi+1)} - \frac{b}{(1+b)(b-a)(b-\xi)}\right]. \tag{2}$$

To find the real and imaginary parts of K, equation (2) is solved, using the transformed boundary conditions. By integrating between points B and D, using Cauchy's Integral theorem [9 (pp. 1–200)], we transform equation (2) as follows

$$\frac{b_2 - (b_1 - b_3)\cos\alpha}{\sin\alpha} + i(b_1 - b_3) = K\pi\left[\frac{1}{(1+a)(1+b)} - \frac{a^{\alpha/\pi}}{(1+a)(b-a)}\cos\alpha + \frac{b^{\alpha/\pi}}{(1+b)(b-a)}\cos\alpha\right]\operatorname{cosec}\alpha \tag{3}$$

The variables b_1, b_2 and b_3 represent the widths of the channels 1, 2 and 3, respectively, as shown in Fig. 1. By denoting $\mathrm{Re}(K) = \mathrm{K}_1$ and $\mathrm{Im}(K) = K_2$, we may separate the real and imaginary parts of equation (3) as follows:

$$b_2 - (b_1 - b_3)\cos\alpha = K_1\pi\left[\frac{1}{(1+a)(1+b)} - \frac{a^{\alpha/\pi}}{(1+a)(b-a)}\cos\alpha + \frac{b^{\alpha/\pi}}{(1+b)(b-a)}\cos\alpha\right] \tag{4}$$

and

$$(b_1 - b_3) = K_2\pi\left[\frac{1}{(1+a)(1+b)} - \frac{a^{\alpha/\pi}}{(1+a)(b-a)}\cos\alpha + \frac{b^{\alpha/\pi}}{(1+b)(b-a)}\cos\alpha\right]\operatorname{cosec}\alpha. \tag{5}$$

Furthermore, considering only the imaginary part, integration of equation (2), from $(a-\epsilon)$ to $(a+\epsilon)$ for point E and from $(b-\epsilon)$ to $(b+\epsilon)$ for point A, such that $\epsilon \to 0$ where ϵ is an infinitesimally small real number, we obtain

$$b_3 = K_1\pi\frac{a^{\alpha/\pi}}{(1+a)(b-a)} \tag{6}$$

and

$$b_1 = K_1\pi\frac{b^{\alpha/\pi}}{(1+b)(b-a)} \tag{7}$$

It now follows that

$$\frac{a^{\alpha/\pi}}{(1+a)b_3} = \frac{b^{\alpha/\pi}}{(1+b)b_1} \tag{8}$$

Substituting equations (6) and (7) in equation (4), we have

$$b_2 - (b_1 - b_3)\cos\alpha = K_1\pi\left[\frac{1}{(1+a)(1+b)} - \frac{a^{\alpha/\pi}(b_3 - b_1)}{b_3(1+a)(b-a)}\cos\alpha\right]. \tag{9}$$

Furthermore, dividing equation (9) by (6), we find

$$\frac{b_2}{b_3} + \left[1 - \frac{b_1}{b_3}\right] \cos\alpha = \left[\frac{(b-a)}{(1+b)a^{\alpha/\pi}} - \frac{(b_3 - b_1)}{b_3} \cos\alpha\right]. \tag{10}$$

Thus, for given values of b_1, b_2, b_3 and α, equations (5), (6), (8) and (10) can be used to calculate a, b, K_1 and K_2.

The velocity vector in the physical plane can be found by relating the sink and source strengths in the complex plane to the velocity potential. The velocity at any point is given by

$$-V_x + iV_y = -\frac{dW}{dZ} = -\frac{dW}{d\xi}\frac{d\xi}{dZ} \tag{11}$$

where W represents the complex velocity potential, V_x represents the velocity component in the x-direction and V_y represents the velocity component in the y-direction. Since the velocity is zero at the stagnation point, the location of the stagnation point is determined by

$$-\frac{dW}{dZ} = 0 \tag{12}$$

To represent the incoming and outgoing flows, consider two sinks of strengths $\frac{V_2 b_2}{\pi}$ and $\frac{V_3 b_3}{\pi}$ at $\xi = -1$ and $\xi = a$ in the complex plane respectively and a source of strength $\frac{V_1 b_1}{\pi}$ at $\xi = b$. V_1, V_2 and V_3 represent the average velocity through channels 1, 2 and 3, respectively. Hence, the complex potential, W is represented as

$$W = \frac{V_2 b_2}{\pi}\log(\xi + 1) + \frac{V_3 b_3}{\pi}\log(\xi - a) - \frac{V_1 b_1}{\pi}\log(\xi - b). \tag{13}$$

By differentiating equation (13), we get

$$\frac{dW}{d\xi} = \frac{V_2 b_2}{\pi(\xi + 1)} + \frac{V_3 b_3}{\pi(\xi - a)} - \frac{V_1 b_1}{\pi(\xi - b)}. \tag{14}$$

This leads to:

$$-\frac{dW}{dZ} = \frac{V_1 b_1(\xi + 1)(\xi - a)}{K\pi\xi^{\alpha/\pi}} - \frac{V_2 b_2(\xi - a)(\xi - b)}{K\pi\xi^{\alpha/\pi}} - \frac{V_3 b_3(\xi + 1)(\xi - b)}{K\pi\xi^{\alpha/\pi}}. \tag{15}$$

Also, to relate the discharge going out through the channel branch with respect to the discharge from the incoming flow, define

$$\eta_q = \frac{V_2 b_2}{V_1 b_1} \tag{16}$$

Furthermore, mass continuity relates the different values of velocities and widths as follows:

$$V_1 b_1 = V_2 b_2 + V_3 b_3. \tag{17}$$

The position of the stagnation point can be found by using equations (12), (16) and (17). For the stagnation point to conincide with the corner, D, the value of ξ must be zero, and the value of the numerator of equation (15) must be equal to zero. In this case, the critical discharge ratio is

$$\eta_{qcr} = \frac{b - a}{b(1 + a)}. \tag{18}$$

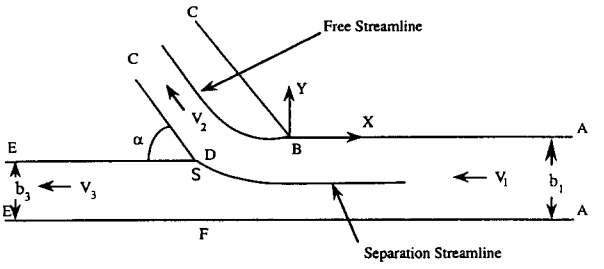

Fig. 3. Physical boundaries of channel junction (stagnation point coincides with corner D) (Z-Plane).

Hence, when the flow splits between channels 1 and 2 in the ratio of η_{qcr} the stagnation point will coincide with point D. For flow ratios greater than η_{qcr}, the stagnation point will be located between points D and C and for flow ratios less than η_{qcr}, between D and E. The position of the stagnation point on the actual physical plane can be obtained by integrating equation (1) between DC or DE, depending on whether the value of η_q is greater than or less than η_{qcr} respectively.

Note that without separation at any point on the boundary as described previously, the velocity at the corner D is infinite. Any fluid flowing past a sharp corner has to seperate from the boundary at the corner. Presence of a finite velocity at the corner can be accounted for by using the free-streamline approach of Helmholtz. Furthermore, as shown earlier, there are three cases to consider, depending on whether the value of η_q is less than, equal to or greater the η_{qcr}. In the subsequent analysis the stagnation point is ar point D.

2.2. Flow with stagnation point at corner, D

The advantage of having a free streamline is that the pressure and hence, the velocity are constant along the free streamline. The free streamline represents a boundary with stagnant fluid behind it. This is consistent with our assumption that the flow is inviscid. In order to determine the location of the free streamline, the Z-plane is transformed onto a Q-plane (Fig. 4a). This is achieved by using the transformation

$$Q = \log\left(\frac{V_2}{V}\right) + i\theta = \log\left\{V_2\left(\frac{\mathrm{d}Z}{\mathrm{d}W}\right)\right\}. \tag{19}$$

Q is an analytic function which transforms the Z-plane on to a straight-edged hodograph plane, Q-plane, thereby simplifying the subsequent calculations. Here V is the magnitude of the velocity vector, i.e., $V = \sqrt{V_x^2 + V_y^2}$. By using the Schwarz-Christoffel transformation to project the flow area on to the positive part of the real axis, we obtain the λ plane, and

$$\frac{\mathrm{d}Q}{\mathrm{d}\lambda} = \frac{K}{\sqrt{\lambda(\lambda+1)}}. \tag{20}$$

The transformation legends are shown in Figs. 3, 4a and 4b. Using the boundary conditions $Q = \pi i$ at $\lambda = -1$ (Point B) and $Q = (\pi - \alpha)i$ at $\lambda = 0$ (Point C), integration of equation (20) gives

$$Q = \left[-\left\{\sqrt{\lambda+1} - \sqrt{\lambda}\right\}^{2\alpha/\pi} e^{-i\alpha}\right]. \tag{21}$$

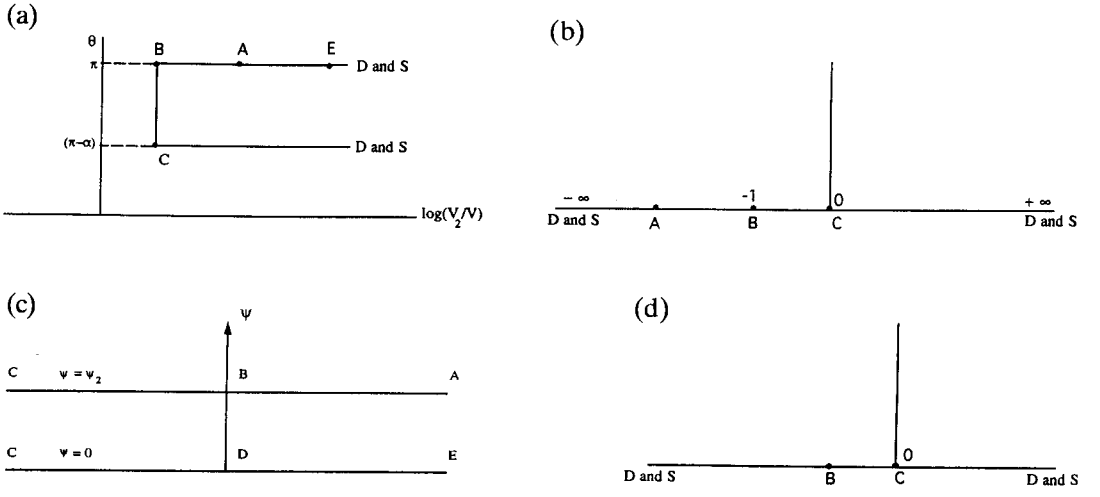

Fig. 4. Transformation layout for locating free-streamline (Stagnation Point S coincides with D). (a) Q-Plane; (b) λ-Plane; (c) W-Plane; (d) λ-Plane.

By comparing equations (19) and (21), we find

$$V_2 \frac{dZ}{dW} = -\cos(\alpha - \alpha_o) + i \sin(\alpha - \alpha_o), \tag{22}$$

where

$$\alpha_o = \frac{2\alpha}{\pi} \arcsin\alpha(\sqrt{-\lambda}). \tag{23}$$

Since the area near the free streamline is of primary interest, it is necessary to relate the corresponding points with their mapped images (Figs. 4c and 4d). The Schwarz-Christoffel transformation leads to

$$\frac{dW}{d\lambda} = \frac{\tilde{k}}{\lambda}, \tag{24}$$

where $\tilde{k}$ is a constant. Integrating about point C from $(0+\varepsilon)$ to $(0-\varepsilon)$, such that $\varepsilon \longrightarrow 0$, we get

$$\tilde{k} = \frac{\Psi_2}{\pi}, \tag{25}$$

where Ψ_2 signifies the rate of discharge per unit width across the diverging branch. Combining equations (22), (23) and (25) we obtain

$$dZ = \frac{\Psi_2}{\pi \lambda V_2} [-\cos(\alpha - \alpha_o) + i \sin(\alpha - \alpha_o)]\, d\lambda, \tag{26}$$

which, when integrated between B and C, yields

$$x = -\frac{b_2}{\pi} \int_{-1}^{-\lambda} \frac{\cos(\alpha - \alpha_o)}{\tilde{\lambda}} d\tilde{\lambda} \tag{27}$$

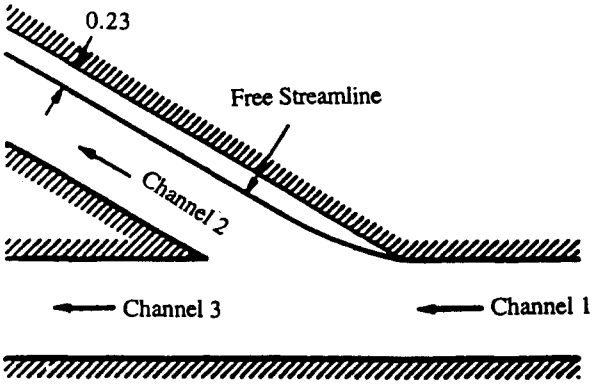

Fig. 5. Streamline plot at angle, $\alpha = 30°$.

and

$$y = \frac{b_2}{\pi} \int_{-1}^{-\lambda} \frac{\sin(\alpha - \alpha_o)}{\tilde{\lambda}} d\tilde{\lambda}. \tag{28}$$

Variables x and y denote the coordinates of the free streamline. The coordinate system is shown in Fig. 3.

3. Applications

To illustrate the applications of the results, assume that channels 1, 2 and 3 have the same width, i.e., $b_1 = b_2 = b_3$. This assumption simplifies equation (8) to

$$\frac{a^{\alpha/\pi}}{1+a} = \frac{b^{\alpha/\pi}}{1+b} \tag{29}$$

Equation (10) reduces to

$$1 = \frac{(b-a)}{(1+b)a^{\alpha/\pi}} \tag{30}$$

Equations (29) and (30) can be solved using the Newton-Raphson scheme for the nonlinear system of ordinary differential equations. Note that if α is 90°, the stagnation point coincides with point D for the same η_{qcr} as the one for converging flows [6]. This observation is expected, because the analysis is inviscid and irrotational. Hence for this particular case, the flow lines are 'similar', whether the flow is diverging or converging, as there is no energy loss taking place.

Equations (29) and (30) are solved for three values of α. Streamline plots are shown in Figs. 5, 6 and 7.

Case 1: $\alpha = 30°$. In this case, a=0.016, b=1.038, and η_{qcr}=0.969. Equations (27) and (28) then yield the free streamline shown in Fig. 5. In Fig. 5, the actual dimensions of the free streamline with respect to the dimensions of the channel are plotted. BCD represents the physical channel boundary (refer Fig. 3). The dimensions of the free streamline increases from 0 (i.e., coinciding at corner B) to an asymptotic value. At the asymptotic end, C, the flow becomes parallel to sides BD and CD.

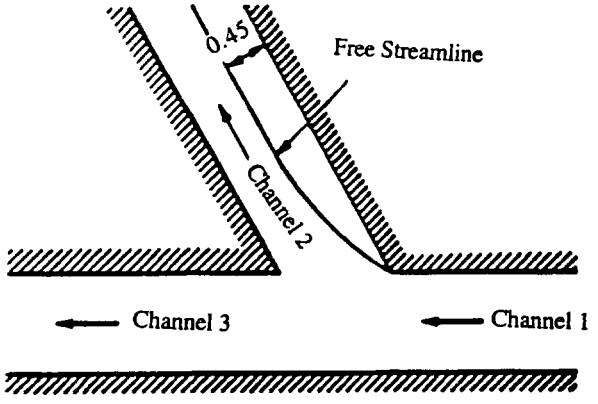

Fig. 6. Streamline plot at angle, $\alpha = 60°$.

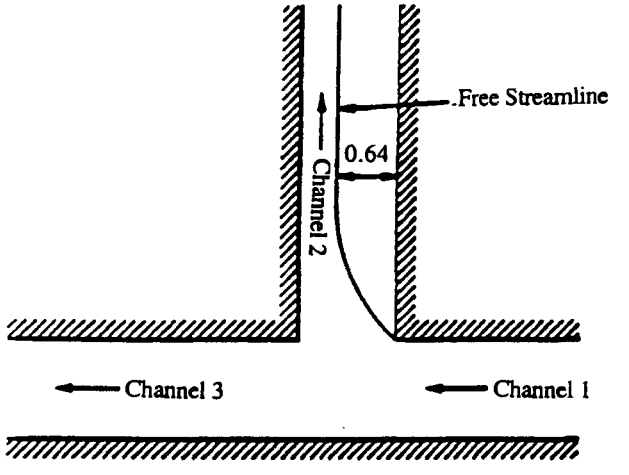

Fig. 7. Streamline plot at angle, $\alpha = 90°$.

Case 2: $\alpha = 60°$. In this case, a=0.149, b=1.452 and η_{qcr}=0.780. The free streamline is plotted in Fig. 6.

Case 3: $\alpha = 90°$. In this case, a=0.382, b=2.618 and η_{qcr}=0.618, and the streamline is as shown Fig. 7.

As expected, the size of the separation zone increases with increasing α. Furthermore, increasing the discharge ratio η_q to a value larger than η_{qcr} results in the shifting of the stagnation point on the side DC. In effect, this will result in the reduction of the width of the separation zone. Similarly, if the discharge ratio η_q is reduced to a value lower than η_{qcr}, the separation zone will be increased in size.

The authors could not find experimental results for the cases when α is not equal to 90°. The separation zone in a 90° branch was measured by Kasthuri and Pundariknathan [10]. They obtained by regression the following relationship between maximum width of separation H and discharge ratio η_q:

$$\frac{H}{b_2} = 0.504\eta_q^2 - 0.893\eta_q + 0.861 \tag{31}$$

Substituting the value of η_{qcr} derived herein, $\eta_{qcr} = 0.618$, we get

$$\frac{H}{b_2} = 0.502 \tag{32}$$

This value is slightly lower than that predicted by the theory, which is $\frac{H}{b_2} = 0.636$ (Fig. 7).

4. Discussion

The above analysis provides a model for calculating the width of the separation zone, utilizing the conformal mapping technique. The analysis however, is expected to over-estimate the width due to the assumptions made in simplifying the analysis. The most important factor contibuting to the difference between the predicted and the actual data is the omission of energy loss at the junction. Also, the fluid behind the free streamline is assumed to be stagnant, which in reality, it is not. In reality, flow behind the free streamline leads to a reduction in pressure within the separation zone and hence, may account for lower values of the width of the separation zone. Use of potential flow theory limits the analysis to flow without vorticities or flows with very low speed. Nonetheless, the potential-flow approach provides insight into the physics of the problem and it provides and alternate theoretical model.

5. Acknowledgement

This work was supported through the Iowa Institute of Hydraulic Research's Electric Power Research in Iowa Program, which is funded by Iowa's Investor-Owned Utilities.

References

1. G. K. Batchelor, *An Introduction to Fluid Dynamics*. Cambridge University Press (1967) pp. 615.
2. G. Kirchhoff, Zur Theorie freier Flüssigkeitsstrahlen. *Crelle's Journal*, 70 (1869) 289–298.
3. H. Rouse (ed.), *Advanced Mechanics of Fluids*., New York: John Wiley & Sons, (1959) pp. 444.
4. J. S. McNown and C. S. Yih, Free streamline analysis of transition flow and jet deflection. University of Iowa, *Bulletin* No. 35 (1953) 1–15.
5. I. G. Currie, *Fundamental Mechanics of Fluids*. New York: McGraw Hill Publishers, (1974).
6. P. N. Modi, P. D. Ariel and M. M. Dandekar, Conformal mapping for channel junction flow. *Journal of Hydraulic Divsion*, ASCE 107 (1981) 1713–1733.
7. R. A. Elder, A. J. Odgaard, V. C. Patel, S. K. Sinha, F. Sotiropoulos and L. Weber, The next generation in three-dimensional hydrodynamic problem solution. *Advances in Hydroscience and Engineering* D. Lianzhen and Sam Y. Wang (eds.), II (1995), 2187–2193.
8. V. Neary, F. Sotiropoulos and A. J. Odgaard, Three-dimensional numerical model of diverging open channel flows. To appear in the proceedings of the American Society of Civil Engineers, *Hydropower -95*, July 1995, San Francisco, USA.
9. R. V. Churchill and J. W. Brown, *Complex Variables and Applications*. New York: McGraw Hill Publishers (1984) pp. 339.
10. B. Kasthuri and N. V. Pundariknathan, Discussion of separation zone at open channel junctions by James L. Best and Ian Reid. *Journal of Hydraulic Engineering*, 113 (1987) 543–544.